



capacitance  $C_p = 740$  pF is largely constant over the operating range, [4]. In combination with the target resonance frequency range, these values yield a comparably low quality factor whose minimal value can reach  $Q_{\min} = 14.5$ . The inductance  $L_p$  can be modified via a magnetization bias current  $I_A$  in order to tune the cavity to some given resonance frequency. Each cavity is equipped with a low-level RF control system (LLRF) which is depicted in Fig. 1 and consists of PI controllers for the amplitude and resonance frequency and a controller of integral type for the phase. Amplitude and phase discriminators are simplified and modeled based on the algorithm presented in [5]. The generator produces the single harmonic cavity driving current  $I_G(t)$  based on the commanded phase and amplitude values of the corresponding controllers.

Finally the beam dynamics are modeled and simulated via a macro particle tracking approach. Herein the state of each particle is discontinuously mapped each turn by the sum of the individual gap voltages.

## SENSITIVITY ANALYSIS

Clearly, the disturbance  $I_B$  lies in the image space of the system input  $I_G$ , see Eq. (1). Given an appropriate estimation or measurement of the disturbance, it is particularly tempting to cancel out its influence via a feed-forward compensation, before the system dynamics are significantly perturbed. However, in the forefront it is unclear how accurate a feed-forward compensation has to be. Thus, in the following we will analyze the sensitivity of the beam dynamics w.r.t. compensation errors by numerical simulations of the longitudinal dynamics of a reference cycle. The results may be particularly useful for defining requirements of both estimations or beam current sensors, when a closed feedback structure is considered.

As no analytic methods do exist to establish any performance criteria or even stability proof, we have to resort to numerical simulations which cover the relevant dynamics described before, to analyze the influence of the compensation. As test case we consider the planned  $^{238}\text{U}^{28+}$  extremum cycle whose essential parameters are summarized in Table 1. This scenario does possess significant beam loading and is therefore particularly interesting for control system validation. At injection the peak beam current is

Table 1: Main Cycle Values, extract from [6]

Parameter	Value	Dimension
ion mass	238.05078	amu
number of ions	$5 \times 10^{11}$	
injection energy	195.7	MeV/u
extraction energy	2700	MeV/u
RF frequency	1.56 - 2.67	MHz
gap voltage (max)	372.53	kV
synchronous phase (max)	59.28	deg
ramping rate (max)	4	T/s
momentum compaction	0.005	

about 1.6 A and rises to 9 A during acceleration. Despite the lower beam current, the injection phase is more sensitive as only two cavities are active providing a summed up gap voltage of 30.55 kV, while the others are running idle. Without counter measures to handle the beam current in the accelerating cavities, this cycle would lead to unstable beam dynamics and complete particle loss.

During stationary operation, i.e. without acceleration, the beam current of a single matched bunch can be well approximated by a Gaussian pulse given by

$$I_B^{\text{SB}}(t) = \hat{I}_B \exp\left(\frac{-t^2}{2\sigma^2}\right),$$

where  $\hat{I}_B$  denotes the peak value of the beam current and  $\sigma$  characterizes its width. Given appropriate measurements or estimations  $\tilde{I}_B$  and  $\tilde{\sigma}$  of the real values  $\hat{I}_B$  and  $\sigma$ , a compensation signal can be synthesized to cancel out the beam current in each cavity. As time synchronization of the compensation can be very cumbersome from an implementation viewpoint, we consider to synchronize the synthetic compensation signal to the zero-crossing of the also synthetic reference gap voltage signal. It is particularly interesting if adequate results can be achieved by this setup as implementation barriers are significantly reduced. On the other hand a pure synthetic compensation signal has the advantage that no sensor noise is directly fed back into the cavity. For each revolution of the bunchtrain we consider the compensation signal

$$I_C = \sum_{i=1}^{10} \epsilon_i \tilde{I}_B \exp\left(\frac{(\tau_{\text{ref}}^i - t)^2}{2\tilde{\sigma}^2}\right), \quad (2)$$

where  $\epsilon_i \in \{0, 1\}$  indicates if the corresponding bunch is filled. The quality of each single bunch can be assessed by the RMS-emittance given by  $\pi\epsilon_i = \pi\sqrt{\sigma_\tau^2\sigma_W^2 - \sigma_{\tau,W}^2}$ , where  $\tau$  and  $W$  are the canonical conjugate phase space coordinates, namely the time and energy deviation of each particle, with respect to the reference particle. In order to be able to evaluate the beam quality of the whole bunchtrain, let us define the quality criterion  $J(t) = 100 \cdot \|\Delta\epsilon_i(t)/\epsilon_i^0\|_\infty$ , with  $\epsilon_i^0 := \epsilon_i(t=0)$ , where  $\|\cdot\|_\infty$  denotes the supremum norm. This criterion corresponds to the worst percentage emittance growth over the bunchtrain. Figure 2 shows the sensitivity of the emittance over time w.r.t. errors of  $\tilde{I}_B$ . It can be observed that around the ideal value of  $\hat{I}_B = 1.6$  A, a large plateau of about 0.4 A exists where the emittance growth stays well below 5%. However, even at  $\tilde{I}_B = 1$  A, corresponding to an error in amplitude of 37.5%, the induced emittance gain is less than 15%. The same non-problematic behaviour can be observed for errors in the compensation width as shown in Fig. 3. Around the ideal value of 31 deg, it is noticeable, that the beam dynamics are more sensitive if the compensation signal is too narrow compared to the real beam current.

However the impacts of the parameter errors are not independent from one another, i.e. the beam quality does not steadily degrade as the true values are left. Figure 4 shows

Content from this work may be used under the terms of the CC BY 3.0 licence (© 2019). Any distribution of this work must maintain attribution to the author(s), title of the work, publisher, and DOI

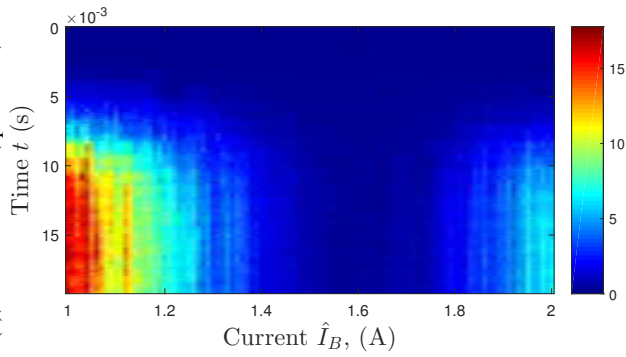


Figure 2: Percentaged emittance growth  $J$  due to amplitude errors of the pre-compensation.

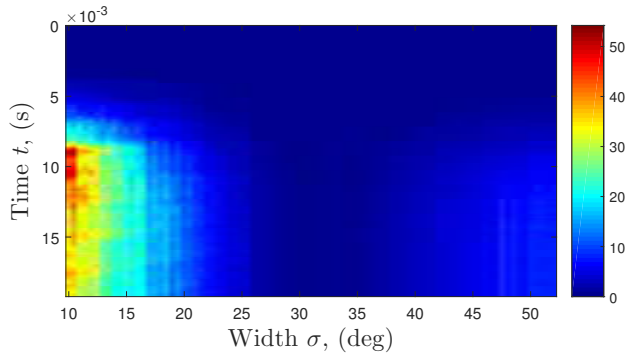


Figure 3: Percentaged emittance growth  $J$  due to width errors of the pre-compensation.

an extensive parameter scan for errors in both height and width of the compensation. The true values are marked by the red cross. A conspicuous feature is the diagonal band of low emittance growth even in the area of considerable errors in the compensation signal. For example the points in the upper right still guarantee an adequate quality with an emittance growth of less than 5%. This phenomenon can be illustrated by regarding the frequency components of the disturbance signal  $I_D = I_B - I_C$ . By using the Fourier transform of the idealized beam current (c.f. [2]) and processing it by the cavity dynamics (1), the average power of the induced stationary disturbance gap voltage signal follows by Parseval's theorem for power signals. Figure 5 shows the normalized analytic disturbance signal power in dependence of the normalized amplitude and width errors. The good qualitative accordance with the numerical results fortify the validity of the approach.

## CONCLUSION AND OUTLOOK

The results of the cycle simulations indicate that feedforward compensation is a valid approach for beam quality improvement. Even though the compensation is synchronized with the reference signal and not the measured beam signal, satisfactory and robust beam dynamics can be achieved. For implementation this result is important as time lag compensation for measured signals can be very cumbersome to achieve. The results can be further improved when a feed-

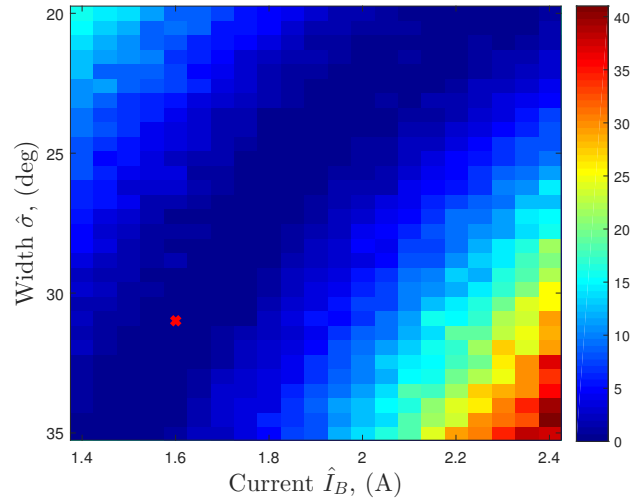


Figure 4: Percentaged emittance growth  $J$  due to amplitude and width errors of the pre-compensation at  $t = 22$  ms.

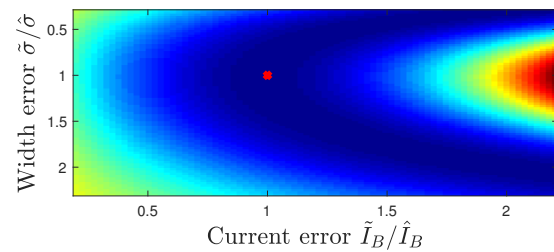


Figure 5: Normalized power of analytic disturbance.

back scheme is considered either by measuring and estimating the beam parameters or by an iterative learning-based control. Finally it has to be emphasized that a beam current compensation does not inflict other counter measures but can be deployed in parallel in order to improve the beam quality. For instance it can drastically reduce the settling time of the LLRF control system when a new bunch is injected into the synchrotron.

## REFERENCES

- [1] D. Mihailescu-Stoica, D. Domont-Yankulova, D. Lens and H. Klingbeil, "On the impact of empty buckets on the ferrite cavity control loop dynamics in high intensity hadron synchrotrons.", IPAC'17, Copenhagen, May 2017.
- [2] D. Mihailescu-Stoica, D. Domont-Yankulova, D. Lens and H. Klingbeil, "cavity impedance reduction strategies during multi cavity operation in the SIS100 high intensity hadron synchrotron.", IPAC'18, Vancouver, May 2018.
- [3] H. Klingbeil, U. Laier, D. Lens, "Theoretical Foundations of Synchrotron and Storage Ring RF Systems", Springer, 2015
- [4] H. König, "Detailed Specification on the SIS100 Acceleration System for FAIR", Tech. rep. GSI, 2013
- [5] P. Händel, "Properties of the IEEE-STD-1057 Four-Parameter Sine Wave Fit Algorithm", IEEE Transactions on Instrumentation and Measurement, Vol. 49, No. 6, December 2000
- [6] D. Ondreka, H. Liebermann, "SIS100 Cycles 5.2", Tech. rep. GSI, 2018